

See discussions, stats, and author profiles for this publication at: <https://www.researchgate.net/publication/236839926>

# Polysiloxane-Based Liquid Crystalline Polymers and Elastomers Prepared by Thiol–Ene Chemistry

ARTICLE *in* MACROMOLECULES · JUNE 2013

Impact Factor: 5.8 · DOI: 10.1021/ma400462e

---

CITATIONS

20

---

READS

129

9 AUTHORS, INCLUDING:



Hong Yang

Southeast University (China)

56 PUBLICATIONS 339 CITATIONS

SEE PROFILE



Patrick Keller

University of Colorado Boulder

61 PUBLICATIONS 2,332 CITATIONS

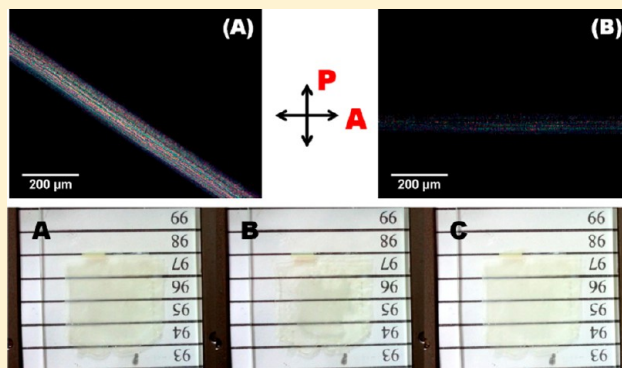
SEE PROFILE

## Polysiloxane-Based Liquid Crystalline Polymers and Elastomers Prepared by Thiol–Ene Chemistry

Hong Yang,<sup>\*,†</sup> Ming-Xia Liu,<sup>†</sup> Yue-Wei Yao,<sup>†</sup> Ping-Yang Tao,<sup>†</sup> Bao-Ping Lin,<sup>\*,†</sup> Patrick Keller,<sup>\*,‡</sup> Xue-Qin Zhang,<sup>†</sup> Ying Sun,<sup>†</sup> and Ling-Xiang Guo<sup>†</sup><sup>†</sup>School of Chemistry and Chemical Engineering, Southeast University, Nanjing 211189, China<sup>‡</sup>Institut Curie, Centre De Recherche, CNRS UMR 168, Université Pierre et Marie Curie, 26 rue d'Ulm 75248 Paris Cedex 05, France

## S Supporting Information

**ABSTRACT:** A series of side-chain liquid crystalline polymers (LCPs) with polysiloxane backbones have been synthesized by grafting mesogenic monomers to poly[3-mercaptopropylmethylsiloxane] (PMMS) via thiol–ene click chemistry. Their properties were studied in detail by a combination of <sup>1</sup>H NMR, gel permeation chromatography, thermogravimetric analysis, differential scanning calorimetry, polarized optical microscopy and small-angle X-ray scattering. In comparison with the traditional hydrosilylation method which requires noble metal catalyst platinum, this newly designed thiol–ene protocol produces polysiloxane-based LCPs with only anti-Markovnikov addition products under benign conditions. Moreover, by controlling the molar ratio of PMMS and mesogenic monomers, PMMS-based LCPs can be partially functionalized, meanwhile leaving spare mercapto groups, which could be further used as cross-linking sites to prepare polysiloxane-based liquid crystalline elastomers (LCEs). Besides preparing LCE fibers with a maximum contraction of 42% at nematic-to-isotropic transition temperature, we further explored the feasibility of using surface-rubbed cells to synthesize LCE films, but it turned out that this method could uniaxially align the mesogens of preformed short polymers but not the backbone chains so that the thermal-actuation effects of these films were modest.



## ■ INTRODUCTION

Liquid crystalline polymers (LCPs) and elastomers (LCEs) have raised up global interests over the past few decades for their wide potential applications as electro-optic or nonlinear optic materials, optical data storage materials, high-strength and high-modulus fibers, engineering plastics, gas separation membranes, stationary phases, artificial muscles, etc.<sup>1,2</sup> Among them, polysiloxane-based LCPs have received extensive attention for their wealth of advantageous physical properties brought by siloxanes. Polysiloxanes possess highly flexible Si–O–Si bonds<sup>3</sup> and excellent permeability<sup>4</sup> as well as low surface energy;<sup>5</sup> they are well recognized as ideal candidates for high-performance elastomers, adhesives, mold release agents, water repellents, protective coatings, and biocompatible materials.<sup>6–10</sup> Thus, combining synergistically the features and characteristics of both siloxanes and liquid crystalline mesogens, can endow the corresponding LCPs with much lower  $T_g$  and viscosities comparing with liquid crystalline polyacrylates, good thermal and mechanical stabilities, etc.

A large variety of polysiloxane-based LCPs and LCEs have been investigated to study their structure–property relationships. The first example was introduced by Finkelmann in 1979,<sup>11,12</sup> and he later invented the famous 2-step-cross-linking process<sup>13</sup> to prepare polysiloxane LCEs, which is the most

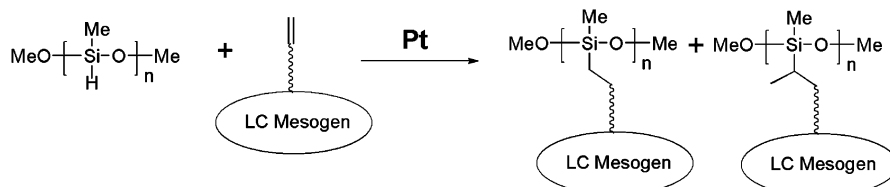
widely used method in the field of LCEs. Percec and his colleagues synthesized a series of side-chain end-on (mesogens are terminally attached) liquid crystalline polysiloxanes bearing macroheterocyclic ligands,<sup>14</sup> half-disk moieties,<sup>15</sup> heterocycloalkanedyl groups,<sup>16,17</sup> and methylstilbene groups.<sup>18,19</sup> Hardouin et al. studied series of side-chain side-on (mesogens are laterally attached) liquid crystalline polysiloxanes or copolysiloxanes, and found that the spacer length, the aliphatic tail length, and the content of mesogenic groups (“dilution” effect) markedly influenced the mesomorphic and thermodynamic properties of these polymers.<sup>20–26</sup> Besides side-chain LCPs, main-chain liquid crystalline polymers (MCLCPs) with mesogenic units and siloxane spacers in the main chain were also reported.<sup>27–29</sup> Recently, Zhou et al. prepared several mesogen-jacketed liquid crystalline polymers (MJLCPs) with polysiloxane backbones and discovered that the mesogen-jacketed effect could force polysiloxanes to self-assemble into supramolecular columnar nematic or smectic liquid crystalline phases.<sup>30</sup> Furthermore, functionalized liquid crystalline polysiloxanes have been applied

Received: March 4, 2013

Revised: April 3, 2013

Published: April 15, 2013

## Traditional Method:



## Our method:

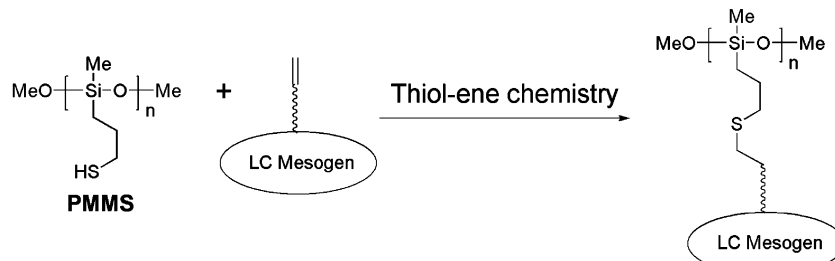


**Figure 1.** Preparation methods of polysiloxane-based liquid crystalline polymers reported previously and herein this manuscript.

as light emitting,<sup>31</sup> ferroelectric,<sup>32–34</sup> gas transportation,<sup>35</sup> and chromatography<sup>36</sup> materials.

Most of the above-reported polysiloxane-based LCPs and LCEs were prepared by hydrosilylation of polymethylhydrosiloxanes with mesogenic alkenes using Pt complex catalysts (Figure 1). However, this traditional method has two disadvantages: (1) this method requires noble metal platinum, which is very expensive and meanwhile is difficult to be removed during the purification procedure; (2) this hydrosilylation reaction usually results in a mixture of Markovnikov and anti-Markovnikov addition products,<sup>37</sup> which might complicate the mesomorphic properties of the corresponding LCPs.

Herein, we present a facile thiol–ene click chemistry method to prepare polysiloxane-based LCPs and LCEs under benign conditions. The thiol–ene addition reaction, as a useful chemical conjugation toolbox, has been widely adopted to synthesize polymeric materials for applications ranging from tissue engineering to dendrimers.<sup>38–45</sup> Inspired by a novel soft lithography technology reported by Hawker et al.,<sup>46,47</sup> we use instead of traditional polymethylhydrosiloxane (PMHS), poly[3-mercaptopropylmethylsiloxane] (PMMS) which possesses one thiol group in every monomer unit as the starting polysiloxane backbone, and graft mesogenic alkenes onto PMMS chain. As shown in Figure 1, this thiol–ene protocol, as a cleaner and greener approach, requires only cheap radical initiators as catalysts, which are much easier to remove during polymer precipitation step; meanwhile the regioselectivity of anti-Markovnikov addition product is almost 100%.

Moreover, we recently reported a two-step sequential thiol–ene click chemistry to prepare thermo-sensitive electrospun fibers bearing PMMS backbone.<sup>48</sup> In this work, we further apply this two-step sequential thiol–ene click chemistry protocol to prepare polysiloxane-based LCEs. As shown in Figure 2, by controlling the molar ratio of PMMS and mesogenic monomers, PMMS-based LCPs can be partially functionalized in the first-step thiol–ene click process, meanwhile leaving spare mercapto groups, which could be further used as cross-linking sites to form LCE networks in the second-step thiol–ene click process.

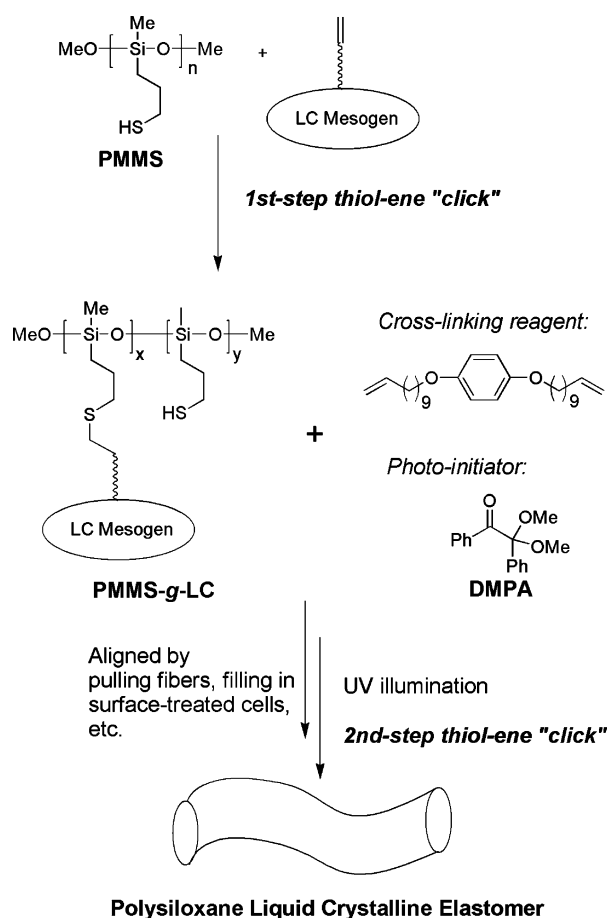


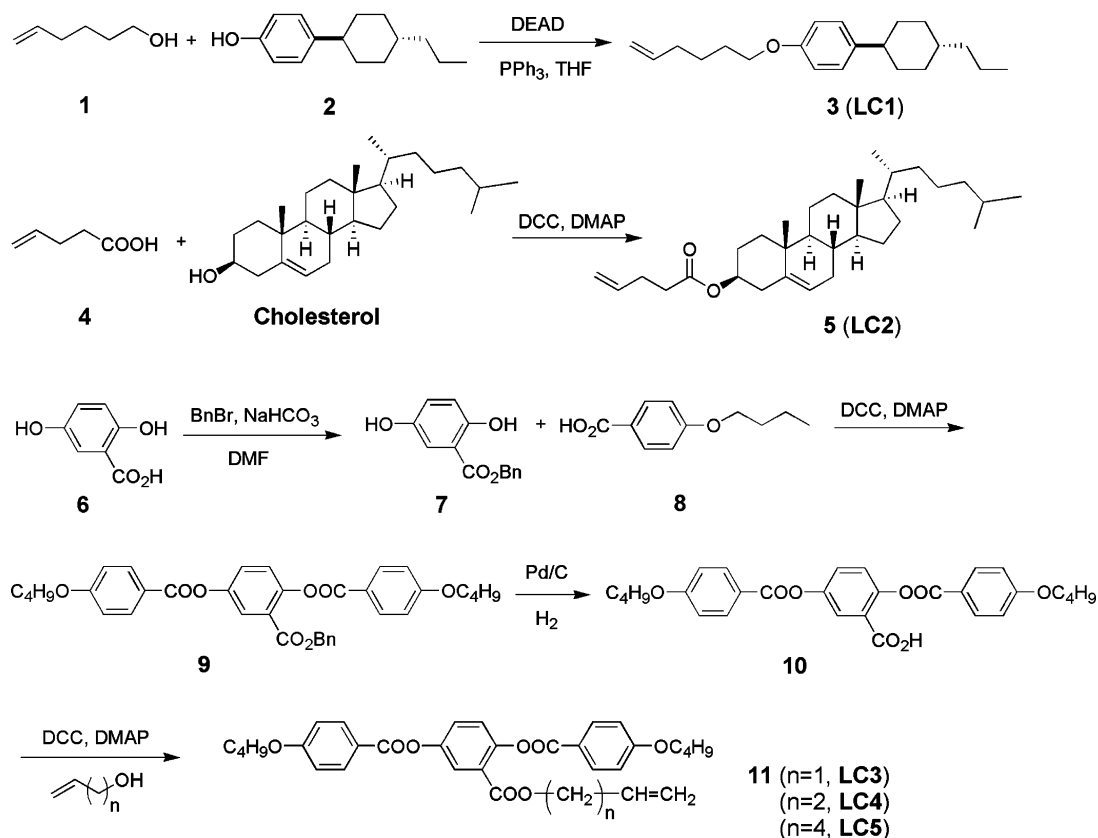
**Figure 2.** Polysiloxane-based liquid crystalline elastomers prepared by a two-step sequential thiol–ene click chemistry protocol.

## EXPERIMENTAL SECTION

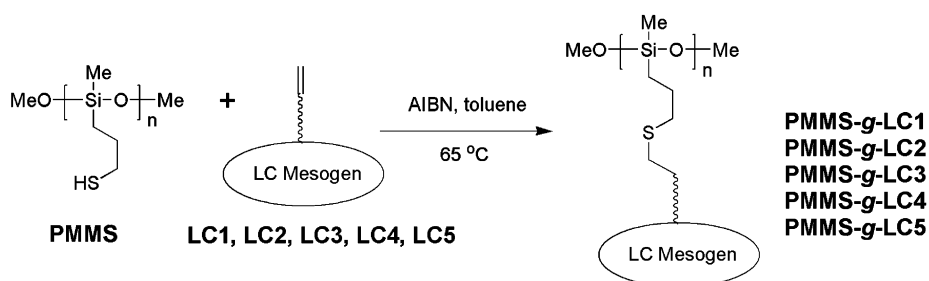
**Materials and Instrumentation.** Poly[3-mercaptopropylmethylsiloxane] (PMMS, SMS-992, M.W. 4000–7000, 95 cst) was purchased from Gelest Inc. 2,2-Dimethoxy-2-phenylacetophenone (DMPA) were purchased from Aldrich Inc. Cholesterol, diethyl azodicarboxylate (DEAD), dicyclohexylcarbodiimide (DCC), and dimethylaminopyr-

Scheme 1. Syntheses of Monomers and Polymers

## Syntheses of Monomers



## Syntheses of Polymers



idine (DMAP) were purchased from aladdin Inc. (Shanghai). Liquid crystal cells were purchased from Instec Inc. Dichloromethane, triethylamine and DMF were distilled from  $\text{CaH}_2$  under nitrogen. THF was distilled from sodium benzophenone ketyl under nitrogen. Other chemical reagents were used without further purification. All nonaqueous reactions were conducted in oven-dried glasswares, under a dry nitrogen atmosphere. All flash chromatography were performed using Macherey-Nagel MN Kieselgel 60 (0.063–1.2 mm).

All  $^1\text{H}$  NMR spectra were obtained using either a Bruker HW500 MHz spectrometer (AVANCE AV-500) or a Bruker HW300 MHz spectrometer (AVANCE AV-300) and recorded in  $\text{CDCl}_3$  (internal reference 7.26 ppm). Gel permeation chromatography (GPC) was performed on an HP 1100 high pressure liquid chromatography (HPLC), equipped with an HP 1047A refractive index detector and a Plgel MIXED-C 300–7.5 mm column (packed with 5  $\mu\text{m}$  particles). The column packing allowed the separation of polymers over a wide molecular weight range of 200–3000000. THF was used as the eluent at a low flow rate of 1 mL/min at 35  $^\circ\text{C}$ . Polystyrene standards were

used as the references. Differential scanning calorimetry (DSC) spectra were recorded on a TA Instruments Q20 instrument (New Castle, DE) under nitrogen purge at a heating rate of 10  $^\circ\text{C}/\text{min}$  from –10 to +130  $^\circ\text{C}$ . Thermogravimetric analysis (TGA) was performed on a Perkin-Elmer TGA7. A UV lamp (20  $\text{mW}\cdot\text{cm}^{-2}$ ,  $\lambda = 365\text{ nm}$ ; LP-40A; LUYOR Corporation) was used to irradiate the samples to perform the photocrosslinking reactions.

Polarized optical microscopy (POM) observations of the liquid crystalline textures of the monomers, polymers and elastomers were performed on an Olympus BX53P microscope with a Mettler PF82HT hot stage. The images were captured using a Microvision MV-DC200 digital camera with Phenix Phmias2008 Cs Ver2.2 software.

X-ray scattering experiments were performed with a high-flux small-angle X-ray scattering instrument (SAXSess, Anton Paar) equipped with Kratky block-collimation system and a temperature control unit (Anton Paar TCS300). At each single steady temperature, both small-angle X-ray scattering (SAXS) and wide-angle X-ray scattering (WAXS) were simultaneously recorded on an imaging-plate (IP)

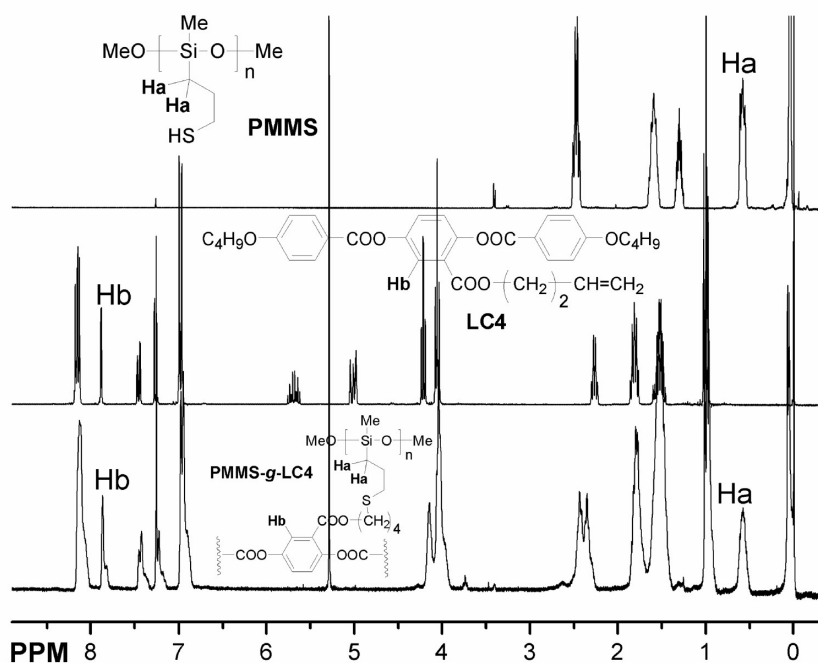


Figure 3.  $^1\text{H}$  NMR spectra of PMMS, LC4, and  $\text{PMMS}_{0.85}\text{-g-LC4}$ .

which extended to high-angle range (the  $q$  range covered by the IP was from 0.06 to  $29\text{ nm}^{-1}$ ,  $q = 4\pi(\sin \theta)/\lambda$ , where the wavelength  $\lambda$  is 0.1542 nm of Cu  $K\alpha$  radiation and  $2\theta$  is the scattering angle) at 40 kV and 40 mA for 30 min.

**Syntheses of Monomers LC1, LC2, LC3, LC4, and LC5.** All the synthetic procedures and  $^1\text{H}$  NMR spectra are listed in the Supporting Information.

**Syntheses of Polymers.** Typical procedure used to prepare  $\text{PMMS-g-LC4}$ : LC4 (364 mg, 0.65 mmol), PMMS (72 mg, 0.54 mmol -SH), AIBN (8.5 mg, 0.05 mmol), and toluene (1.5 mL) were added into a Schlenk-type flask. The flask was degassed and exchanged with nitrogen via three freeze–thaw cycles. The reaction mixture was heated to  $65\text{ }^\circ\text{C}$  for 24 h. The reaction mixture was then poured into methanol (50 mL) to precipitate the polymer. The resulting brownish polymer was further purified by dissolving in THF, reprecipitating from methanol several times, and drying in vacuo, which gave the desired polymer (350 mg; yield 93%) as a milky oil.

**Syntheses of  $\text{PMMS}_{0.85}\text{-g-LC4}$ .** LC4 (258 mg, 0.46 mmol), PMMS (72 mg, 0.54 mmol -SH), AIBN (8.5 mg, 0.05 mmol), and toluene (1.5 mL) were added into a Schlenk-type flask. The flask was degassed and exchanged with nitrogen via three freeze–thaw cycles. The reaction mixture was heated to  $65\text{ }^\circ\text{C}$  for 24 h. The reaction mixture was then poured into methanol (50 mL) to precipitate the polymer. The resulting brownish polymer was further purified by dissolving in THF, reprecipitating from methanol several times, and drying in vacuo, which gave the desired polymer (300 mg; Yield: 91%) as a milky oil.

**Preparation of LCE Fibers.**  $\text{PMMS}_{0.85}\text{-g-LC4}$  (100 mg, 0.025 mmol free -SH theoretically), 1,4-di-11-undeceneoxybenzene<sup>49</sup> (cross-linker, 5 mg, 0.012 mmol), and 2,2-dimethoxy-2-phenylacetophenone (photoinitiator, 0.64 mg, 0.0025 mmol) were added into a 5 mL vial. The mixture was fully dissolved in 1 mL of dry  $\text{CH}_2\text{Cl}_2$ , the solvent was then removed in vacuo. The vial was placed on a hot stage and heated to  $80\text{ }^\circ\text{C}$ . When the mixture became viscous, the fibers were drawn by dipping the tip of a capillary pipet and pulling the mixture with it as quickly as possible. The fibers were then placed on a microscope slide which has been surface-treated with several drops of silicone oil to prevent fibers to stick on the glass. The microscope slide was placed on a hot stage and heated to  $40\text{ }^\circ\text{C}$  which is in the liquid crystalline phase. At  $40\text{ }^\circ\text{C}$ , the fibers were irradiated by

using a UV-lamp for 30 min. The average diameter of the fiber prepared this way was about  $90\text{ }\mu\text{m}$ .

**Preparation of LCE films.** The above mixtures of  $\text{PMMS}_{0.85}\text{-g-LC4}$ , 1,4-di-11-undeceneoxybenzene, and 2,2-dimethoxy-2-phenylacetophenone were used in the preparation of aligned LCE films. Mixtures, heated in their isotropic phase ( $100\text{ }^\circ\text{C}$ ), were filled by capillarity in rubbed polyimide-coated glass cells of  $20\text{ }\mu\text{m}$  gap (commercial Instec LC cells). The filled cells were slowly cooled down at  $-1\text{ }^\circ\text{C}/\text{min}$  to the nematic phase of the mixture to achieve planar alignment. The cooling and the subsequent UV irradiation were carried under a stream of nitrogen (using a zip-lock bag<sup>41,50</sup>), to ensure an inert atmosphere during the radical polymerization. After UV irradiation ( $365\text{ nm}$ ,  $20\text{ mW}/\text{cm}^2$ ) for 0.5 h, the free-standing, aligned LCE films were obtained by dissolving the glass windows of the cells with 40% aqueous hydrofluoric acid solution.

## RESULTS AND DISCUSSION

**Syntheses and Mesomorphic Properties of Monomers and Polymers.** In order to verify the feasibility of preparing liquid crystalline polysiloxanes by grafting vinyl-terminated mesogens onto PMMS backbone, we designed five different liquid crystalline monomers including two end-on vinyl-terminated mesogens and three side-on vinyl-terminated mesogens. The synthetic protocols of monomers and the corresponding polymers are shown in Scheme 1. The two end-on mesogens, LC1 and LC2, were straightly prepared in one simple step by the standard Mitsunobu etherification reaction<sup>51</sup> and DCC/DMAP esterification reaction<sup>52</sup> respectively. The side-on mesogens, LC3, LC4, and LC5, were synthesized by DCC/DMAP esterification of a previously reported compound  $10^{53}$  and vinyl-terminated alcohols with different alkyl lengths. The corresponding polymers,  $\text{PMMS-g-LC}$ , were prepared by a radical-initiated thiol–ene addition reaction of PMMS and vinyl-terminated mesogens LC1–5 in toluene. Herein,  $\text{PMMS}_{0.85}\text{-g-LC4}$  represents a polymer with 85% of mercapto groups of PMMS having been grafted with LC4 mesogen.

$^1\text{H}$  NMR spectra and the corresponding peak assignments of the commercially available polymer PMMS, a representative



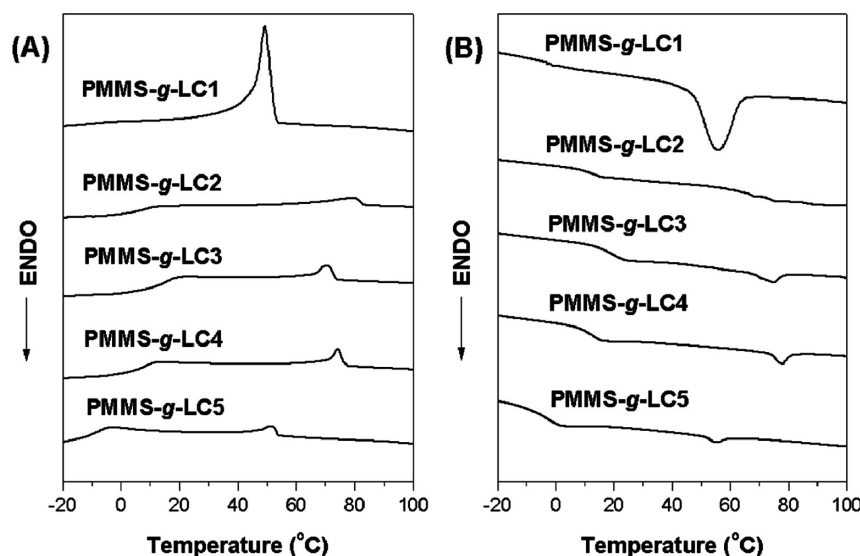


**Figure 4.** DSC curves of PMMS-g-LC during (A) the first cooling scan and (B) the second heating scan at a rate of 10 °C/min under nitrogen atmosphere.

monomer LC4 and a corresponding unsaturated polymer PMMS<sub>0.85</sub>-g-LC4 are shown in Figure 3. In comparison, the terminal olefin protons of LC4 originally located at 5.0–5.7 ppm, as well as the methine proton of S–H bond of PMMS appearing at ~1.3 ppm all disappeared, which proved a successful grafting reaction and implied that all the unreacted monomers have been removed. By measuring the integral ratio of the methylene protons (Ha ~ 0.6 ppm, Si–CH<sub>2</sub>–) of PMMS and the aromatic proton (Hb ~ 7.8 ppm) of LC4, we can roughly calculate the graft density. For example, we designed an unsaturated polymer, PMMS<sub>0.85</sub>-g-LC4, by feeding the monomer LC4 in an 85% molar equivalent of –SH groups of PMMS. On the basis of the integral ratio of Hb and Ha peaks (see the detailed integrations in the Supporting Information), the actual graft density was around 85%, which was a perfect match with the designed scenario. Thus, we can conclude that thiol–ene click chemistry is an efficient method to graft mesogens onto polysiloxane chains and that it is possible to accurately control the graft densities by simply mixing the functional polysiloxane with monomers in desired molar ratios.

These successful grafting results were further confirmed by gel permeation chromatography (GPC). On the basis of our GPC experiments shown in Figure S1, Supporting Information, the polymer precursor, PMMS is a mixture of short oligomers with the major  $M_n$  peak value around 1500 g/mol, though the merchant label said that  $M_n$  value was 4000–7000. The degree of polymerization (D.P.) was thus estimated as below 30. Consequently, all the PMMS-g-LC polymers are short oligomers with a broad polydispersity.

The thermal properties of this new class of polysiloxane-based LCPs were investigated by TGA and DSC. As shown in Figure S2, Supporting Information, the temperatures at 5% weight loss ( $T_d$ ) of the samples under N<sub>2</sub> are all over 300 °C, indicating that all the polymers had good thermal stabilities. Benefiting from their polysiloxane backbones, all these LCPs have really low glass transition temperatures ( $T_g$ ) below 20 °C (Figure 4). Besides glass phase transitions, these five polysiloxane-based LCPs present only one other phase

transition, which is the clearing point of liquid crystalline mesophase-isotropic transition.

The mesomorphic behaviors of all the monomers and polymers PMMS-g-LC were first investigated by POM. The thermal transitions and phase properties of these two series of monomers and polymers are listed in Table 1. All the

**Table 1. Mesomorphic Properties of the Monomers and Polymers<sup>a</sup>**

monomer	phase transitions (°C)	polymer	phase transitions (°C)
LC1	N 25 I I 24 N	PMMS-g-LC1	SmX 62 I I 59 SmX
LC2	K 86 N* 112 I I 110 N* 59 K	PMMS-g-LC2	SmX 82 I I 80 SmX
LC3	K 110 N 133 I I 132 N 85 K	PMMS-g-LC3	N 70 I I 68 N
LC4	K 101 N 115 I I 113 N 79 K	PMMS-g-LC4	N 73 I I 71 N
LC5	K 69 N 95 I I 92 N 46 K	PMMS-g-LC5	N 56 I I 54 N

<sup>a</sup>Detected only by polarized optical microscopy. K = crystalline, N = nematic, N\* = cholesteric, SmX = undefined smectic, I = isotropic, and G = glass phase. First line obtained on heating; second line obtained on cooling.

monomers show enantiotropic nematic phases, and LC2, in particular, presents chiral nematic (cholesteric) phase. Although sharing the same mesogenic core, LC3, LC4, and LC5 have different side-on alkyl tail lengths, which dramatically influence the melting points and clearing points. As long as the side-on tail length increases, both the melting point and clearing point decrease.

In agreement with DSC results, all these polysiloxane-based LCPs have one single enantiotropic liquid crystalline phase from room temperature up to their clearing points under POM observations. As shown in Figure 5 (A and B), PMMS-g-LC1 and PMMS-g-LC2 both exhibit some tiny broken fan-shaped textures, indicative of the presence of a smectic mesophase. On the contrary, PMMS-g-LC3, PMMS-g-LC4, PMMS-g-LC5, and PMMS<sub>0.85</sub>-g-LC4 present the coexistence of thread-like

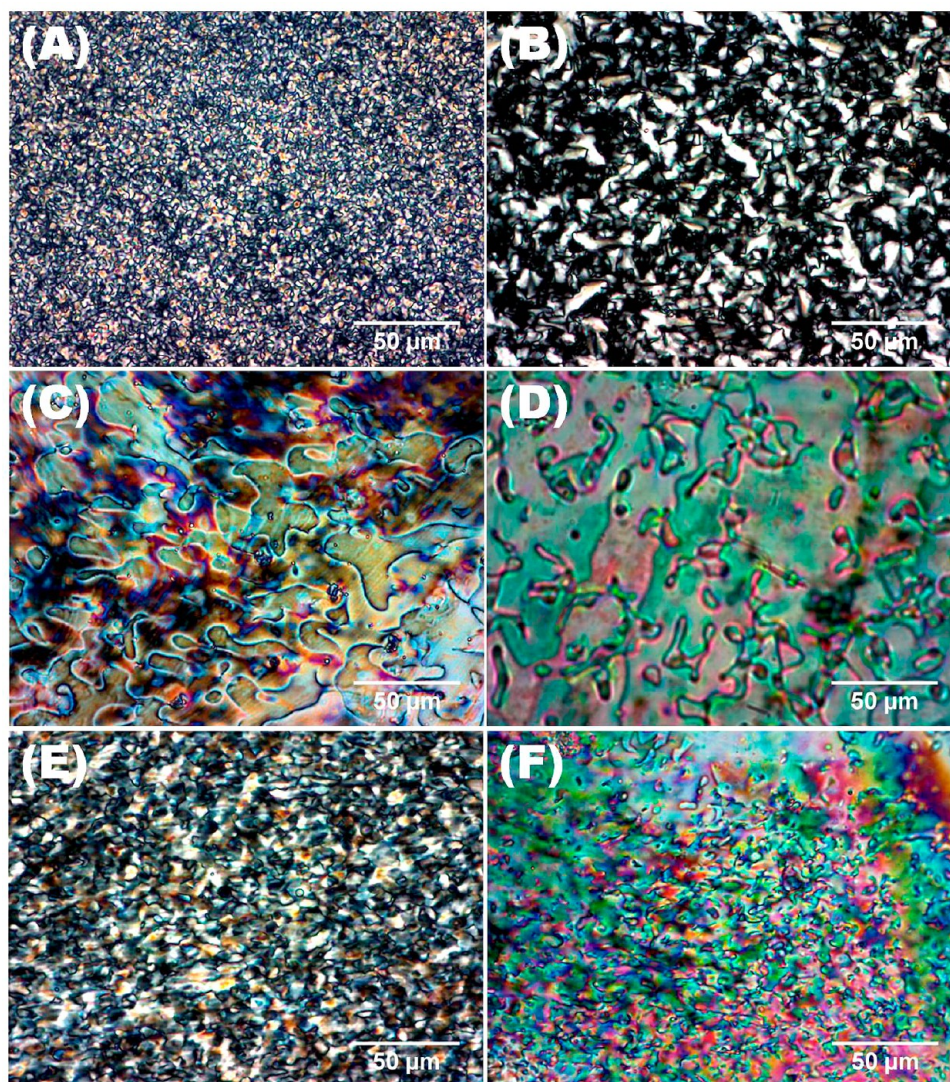


**Figure 5.** Polarized optical microscope images of (A) PMMS-g-LC1 maintained at 50 °C, (B) PMMS-g-LC2 maintained at 60 °C, (C) PMMS-g-LC3 maintained at 60 °C, (D) PMMS-g-LC4 maintained at 60 °C, (E) PMMS-g-LC5 maintained at 40 °C, and (F) PMMS<sub>0.85</sub>-g-LC4 maintained at 50 °C.

textures and marble textures, which are solid proofs of nematic phases.

To confirm the nature of the liquid crystalline phases for these PMMS-g-LC polymers exhibiting birefringent textures, simultaneous SAXS and WAXS were further performed. As presented in Figure 6, the SAXS and WAXS profiles of PMMS-g-LC1 and PMMS-g-LC2 both show three sharp scattering peaks at low angles. At wide angle regions, PMMS-g-LC1 has a sharp peak due to the crystallization of the alkyl tails, while PMMS-g-LC2 has a diffuse peak which demonstrates that the positions of mesogens in a single layer are highly disordered. The reciprocal spacing ratios of these two pairs of three sharp peaks are 1: 1/2: 1/3; hence the peaks can be indexed as (100), (200), and (300) reflections of the lamellar layers, which confirm the existence of smectic phases. The corresponding lamellar thicknesses of PMMS-g-LC1 and PMMS-g-LC2 are 2.91 and 5.66 nm, respectively. Comparing with the fully extended lengths ( $l = 2.87$  nm, 3.10 nm) of the laterally attached mesogens, as estimated by Dreiding models, PMMS-g-LC1 and PMMS-g-LC2 might have SmA and interdigital SmA<sub>d</sub><sup>54,55</sup> phases, respectively, although we lack of 2D WAXD

techniques to precisely define these smectic structures. On the contrary, the SAXS and WAXS patterns of PMMS-g-LC3 and PMMS-g-LC4 both show two diffuse peaks at low angles and wide angles, which further verify the existences of nematic phases.

**Preparation and Thermo-Actuation Properties of LCEs.** Liquid crystalline elastomers (LCE) have been intensively investigated<sup>56–58</sup> during the past two decades, due to their fascinating abilities to change their shapes reversibly under external stimuli (thermal,<sup>59</sup> light,<sup>60,61</sup> electrical,<sup>62</sup> magnetic,<sup>63</sup> etc.) and potential applications as mechanical actuators,<sup>64</sup> chemical sensors,<sup>65</sup> artificial organs,<sup>66</sup> smart surfaces,<sup>67,68</sup> and miniaturized devices.<sup>69–72</sup> The actuation behaviors of LCEs are induced by the anisotropic-isotropic deformation of polymer chains driven by the order transitions of the mesophases. To achieve actuation effects, the mesogens and backbone chains of LCEs have to be aligned uniaxially by mechanical forces, surface effects, electric fields or magnetic fields. The most widely used method was the 2-step-cross-linking process introduced by Finkelmann,<sup>11–13</sup> which performs a partial cross-linkage of polymers first, then applies



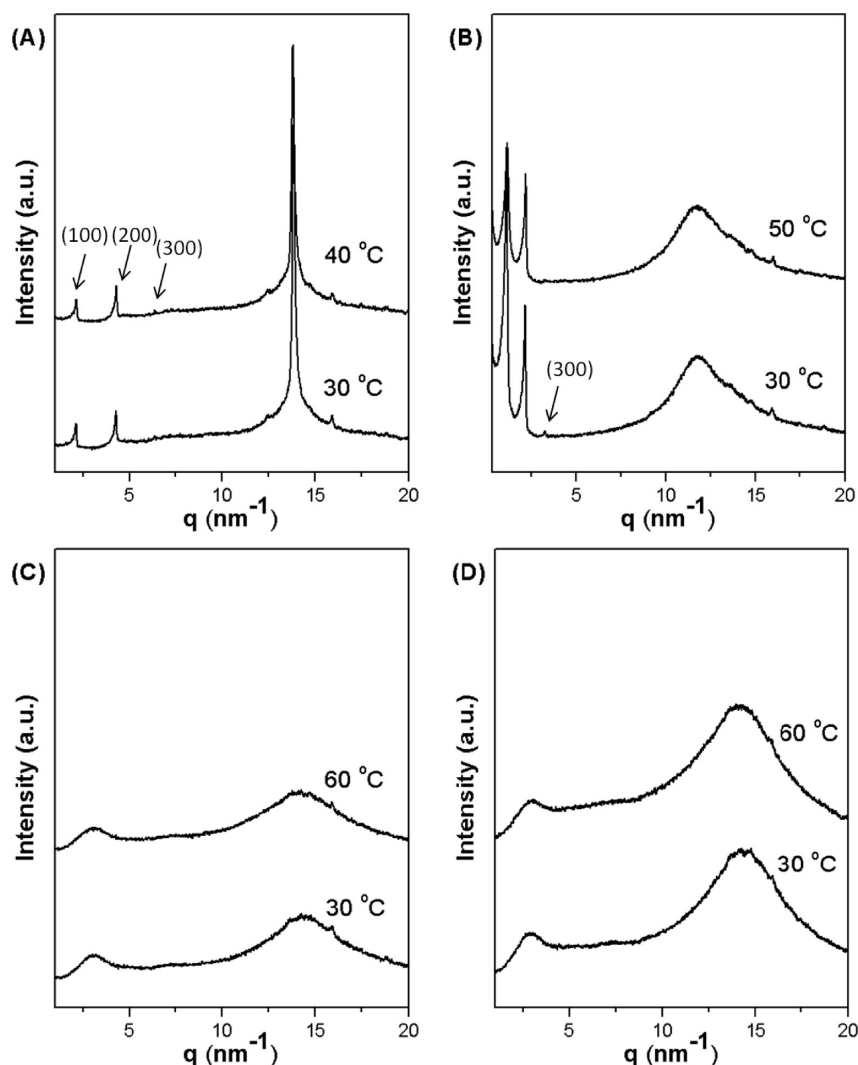


Figure 6. SAXS and WAXS profiles of (A) PMMS-g-LC1, (B) PMMS-g-LC2, (C) PMMS-g-LC3, and (D) PMMS-g-LC4.

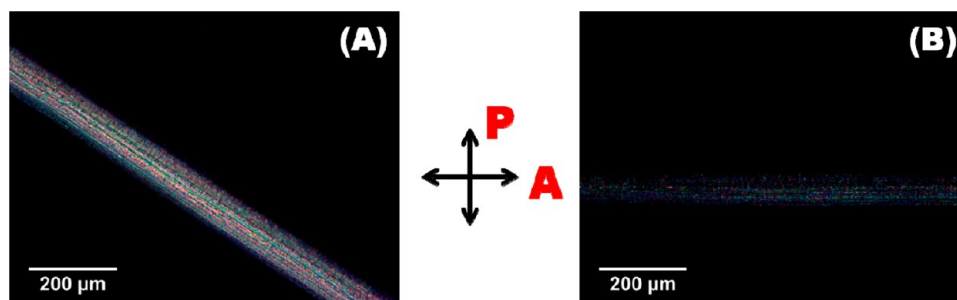


Figure 7. Photomicrographs of a hand-pulled LCE fiber at room temperature between crossed polarizer and analyzer.

mechanical stress to align the samples in anisotropic order, and finally exerts a fully cross-linking to prepare LCEs. Another well-known method was to fill mixtures of liquid crystalline monomers and cross-linkers into antiparallel surface-rubbed cells<sup>53,73</sup> which use surface anchoring effects to align the mesogens and the corresponding cross-linked elastomer backbones in anisotropic order. Although the latter method is very convenient for preparing LCEs starting from small molecules, there were barely any reports using this protocol to directly align functional LCPs to synthesize LCEs probably due to the high viscosities of polymers which make it extremely

difficult to fill polymers into cells by capillarity. Herein in our case, these novel **PMMS-g-LC** polymers are short oligomers with low viscosities, which are able to be filled into liquid crystal cells. Thus, it provided us a good opportunity to explore the feasibility of using antiparallel surface-rubbed cells to directly align functional LCPs and synthesize the corresponding LCE films, which is actually more important to us than developing a new synthetic method to prepare LCPs and LCEs described in the previous parts of this manuscript.

Following the published protocol,<sup>74,75</sup> we prepared at first some hand-pulled LCE fibers as described in the Experimental



Section. As indicated in Figure 7B, the fiber shows excellent extinction when the fiber axis is parallel or perpendicular to the polarizer. Rotation of the fiber by 45° from extinction maximizes the transmission (Figure 7A).

The thermal-actuation properties of these LCE fibers were investigated by following the length of the fiber long axis as a function of temperature. As shown in Figure 8A,B, the fiber

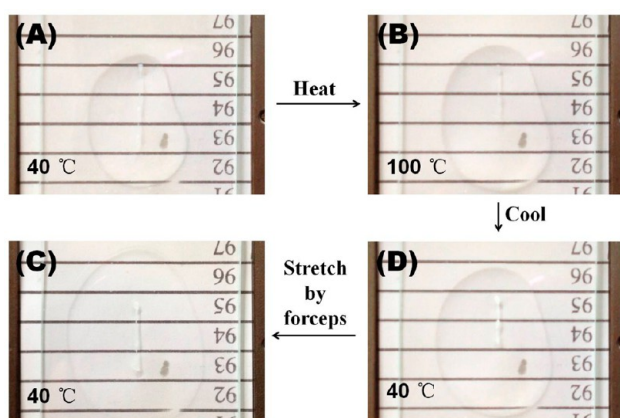


**Figure 8.** Images of a LCE fiber heated from 40 °C (A) to 100 °C (B), then cooled back to 40 °C (C) and stretched by forceps at 40 °C (D).

sample was heated into the isotropic phase on a hot-stage at a slow rate of 1 °C/min and an obvious contraction phenomena was observed (see Film1 in Supporting Information). The spontaneous deformation,  $L/L_{\text{iso}}$  ( $L$  is the length of the fiber at any specific temperature,  $L_{\text{iso}}$  is the length of the fiber in the isotropic state), is plotted in Figure S3, Supporting Information. A maximum shape variation of 42% was achieved in the nematic–isotropic transition range from 73 to 97 °C. Upon cooling back to 40 °C, the fiber sample did wrinkle (Figure 8C) instead of spontaneously expanding to the original formation. A forceps was applied to gently pull the fiber along the long axis and a partial length reversion of the fiber was achieved (Figure

8D). We believe that a full length reversion could be realized if constantly providing an external force during the cooling process following Zentel's protocol.<sup>76,77</sup> Although this mechanical stress process made very nice alignments of polysiloxane-based LCEs, due to the LCPs' low viscosities, these LCE fibers with an average diameter of 90 μm were very thin which greatly narrowed the possible applications as actuators or artificial muscle fibers. Thus, uniaxially aligned polysiloxane-based LCE films became our highly desirable alternatives.

The detailed preparation procedure of polysiloxane-based LCE films using antiparallel surface-rubbed cell alignment method is described in the Experimental Section. Before performing this experiment, our major concern was the cell opening step using aqueous HF solution which might destroy not only the glasses but also the polysiloxane-based LCE films. Encouraged by the superhydrophobic surface properties of polysiloxane-based materials as well as the example of HF etching glass microchannels confined by PDMS molds,<sup>78</sup> we discovered that our polysiloxane-based LCE films could survive in HF for a period of time. A 40% aqueous hydrofluoric acid solution could “eat up” 1.0 mm thick glasses in 20 h, when the polysiloxane-based LCE films were peeled off successfully. However, if the time period was lengthened to 48 h, these LCE films became dark yellow in appearances and were soft, sticky, which implied the elastomer networks have been seriously damaged by HF at longer reaction time.

Under POM observation, the prepared LCE film was well aligned. As shown in Figure 9A,B, the stripe lines represent the surface-rubbed direction. When the stripe direction is 45° from the polarizer, the birefringent textures are very uniform and the transmission maximizes. Rotation of the film with the stripe direction parallel to the polarizer minimizes the transmission although a full extinction of birefringence is not visualized.

The thermal-actuation properties of LCE film were investigated by following the length of the film in surface-rubbed direction as a function of temperature. As shown in Figure 10A–C, the film sample was heated into the isotropic phase on a hot-stage at a slow rate of 1 °C/min which might

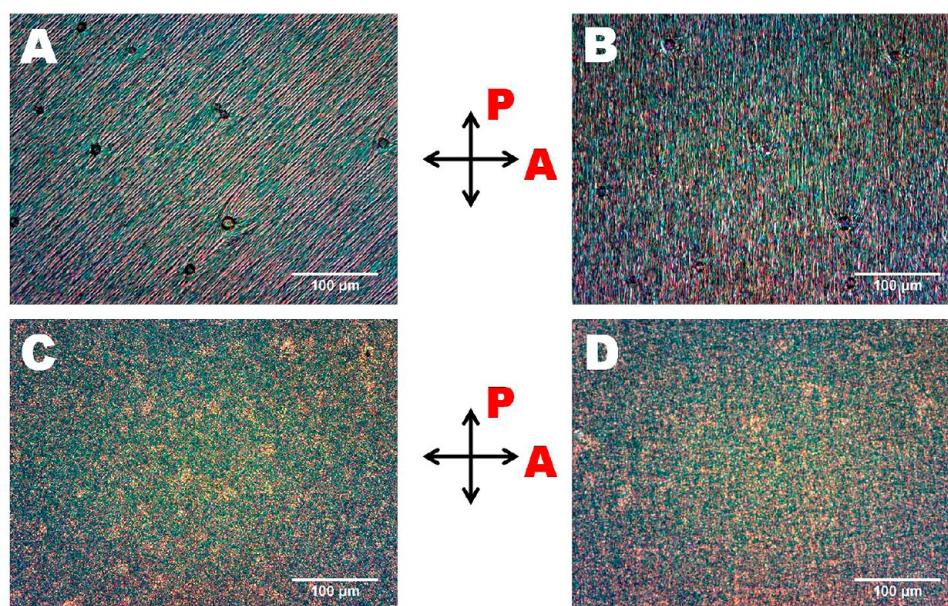


**Figure 9.** Photomicrographs of a LCE film prepared by the antiparallel surface-rubbed cell (A, B) and a LCE film prepared by the nonsurface-treated cell (C, D) at room temperature between crossed polarizer and analyzer.

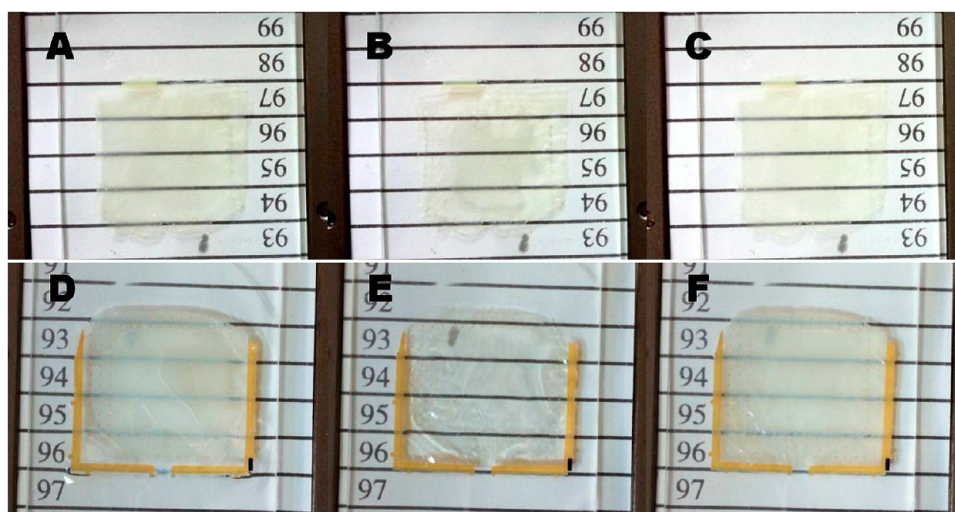


**Figure 10.** Images of LCE films in comparison. The LCE film prepared by the antiparallel surface-rubbed cell, floating on silicone oil, was heated to (A) 40 and (B) 100 °C, and then cooled back to (C) 40 °C. The LCE film prepared by the nonsurface-treated cell, floating on silicone oil, was heated to (D) 40 and (E) 100 °C, and then cooled back to (F) 40 °C. The yellow stripe edges are the glued 20  $\mu\text{m}$  thick spacers.

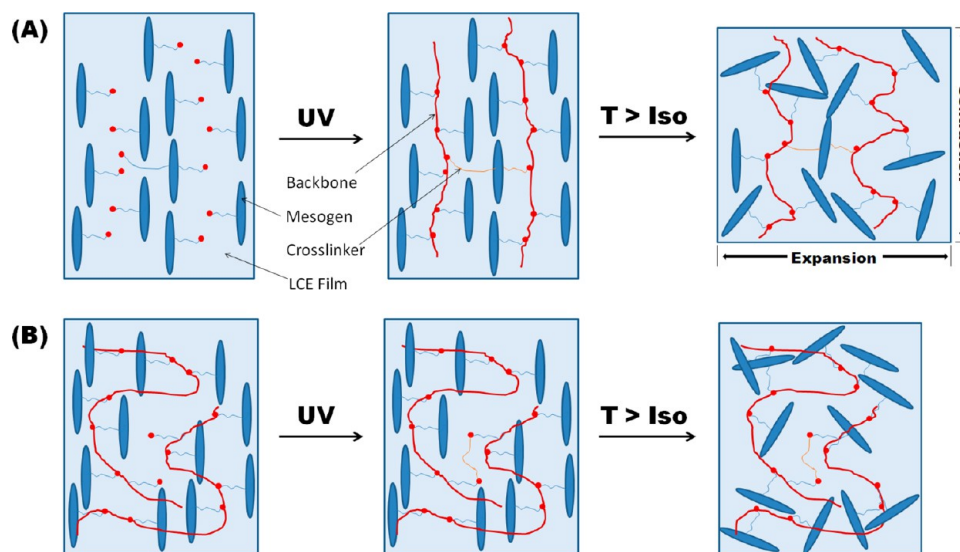


**Figure 11.** Schematic explanation of preparations and thermal-actuation behaviors of LCE films using the antiparallel surface-rubbed cell alignment method, starting from (A) small mesogenic monomers or (B) preformed short liquid crystalline polymers.

minimize effects caused by slow relaxation processes. To our surprise, the reversible thermal-actuation effect was modest, with a maximum shape variation of less than 5%. Film2 in the Supporting Information shows this experiment. However, it is an obvious conflict to our common knowledge since the mesogens are aligned in a fine order based on POM results. To further verify whether the mesogens of LCE film were aligned uniaxially, we performed two experiments in comparison.

First, we used the same type of liquid crystal cells to prepare LCE films starting from liquid crystalline acrylate monomers following the reference work,<sup>53</sup> and realized around 35% reversible actuation as same as the reported scenario (see Film3 in Supporting Information). This experiment proved the quality of these liquid crystal cells, which are capable of aligning LC mesogens.

Second, we filled the sample mixture into a nonsurface-treated cell and UV-illuminated it to prepare a LCE film. As shown in Figure 9C,D, there were no alignments at all under POM observation. Consequently, the film appeared opaque

(Figure 10D,F) when the temperature was below N-Iso transition, because the LC mesogens without alignment would spontaneously form micrometer-sized multidomain areas, which would scatter the light and lower the transmission. When the temperature was raised to above N-Iso transition, all the molecules would be randomly oriented and light scattering phenomena would vanish. Thus, the film appeared transparent (Figure 10E). On the contrary, the polysiloxane-based LCE film prepared by the antiparallel surface-rubbed cell presented almost the same light transmissions at below or above the N-Iso transition temperatures (Figure 10A-C), which proved that the mesogens of LCE film were aligned uniaxially.

A possible reason behind the modest thermal-actuation effect could be that the antiparallel surface-rubbed cell alignment method can only align the mesogens of the preformed short polymers (oligomers) but not the backbone chains, which are still randomly coiled, so that the anisotropic-isotropic transition of laterally attached mesogens will not change the conformations of the backbone chains. As shown in Figure 11A, when



small UV-active mesogenic monomers are filled in an antiparallel surface-rubbed cell, the surface anchoring effect will align all the molecules uniaxially. The subsequent UV-illumination will perform photopolymerization and photocross-linking at the same time. The order of mesogens will force the backbone chains to form in a stretched orientation. Thus, when the corresponding LCE film is heated to above the N-Iso transition temperature, the disordered mesogens will force the macromolecular chains from stretched to coiled, so that an obvious film contraction along the surface-rubbed direction and an expansion along the perpendicular direction are realized. Contrarily, as shown in Figure 11B, when cross-linkable polymers are filled in an antiparallel surface-rubbed cell, the surface anchoring effect can align the laterally attached mesogens uniaxially, but maybe is not strong enough to stretch the backbones to an extended conformation, so that the backbone chains always remain randomly coiled before and after the photocrosslinking process. Thus, when the corresponding LCE film is heated to above the N-Iso transition temperature, the already-coiled conformation of macromolecular chains will not help on changing the film shape dramatically.

## CONCLUSION

In summary, we developed and studied a series of side-chain end-on and side-on liquid crystalline polymers (LCPs) bearing polysiloxane backbones. These novel polymers have been synthesized by grafting mesogenic monomers to poly[3-mercaptopropylmethylsiloxane] (PMMS) via thiol-ene click chemistry. In comparison with the traditional hydrosilylation method which requires noble metal catalyst platinum, this newly designed thiol-ene protocol can prepare polysiloxane-based LCPs with anti-Markovnikov products formed only under benign conditions. On the basis of the POM, DSC, SAXS and WAXS results, we can conclude that these polymers could readily achieve a wide variety of liquid crystalline phases in correspondence to the grafted mesogenic molecular structures.

Moreover, by controlling the molar ratio of PMMS and mesogenic monomers, PMMS-based LCPs can be partially functionalized, meanwhile leaving spare mercapto groups, which could be further used as cross-linking sites to prepare polysiloxane-based liquid crystalline elastomer (LCE) fibers and films. Because of the low viscosities of PMMS-based LCPs, the hand-pulled LCE fibers with an average diameter of 90  $\mu\text{m}$  were very thin, which greatly narrowed the future possible applications. Besides preparing LCE fibers with a maximum contraction of 42% at nematic-to-isotropic transition temperature, we further explored the feasibility of using antiparallel surface-rubbed cells to align and synthesize polysiloxane-based LCE films, which turned out this traditional method could only align the mesogens of preformed short polymers but not the backbone chains so that the thermal-actuation effects of these films were modest. We hope this interesting discovery will present some useful information to the liquid crystal community.

## ASSOCIATED CONTENT

### Supporting Information

General considerations, synthetic procedures and  $^1\text{H}$  NMR spectra, Figure S1, GPC chromatograms of PMMS-g-LC, Figure S2, TGA spectra of PMMS-g-LC, and Figure S3, thermal-actuation properties of PMMS<sub>0.85</sub>-g-LC4 LCE fiber and

three films of LCE samples in .avi format. This material is available free of charge via the Internet at <http://pubs.acs.org>.

## AUTHOR INFORMATION

### Corresponding Author

\*(H.Y.) Telephone: 86 25 52090620. Fax: 86 25 52090616. E-mail: [pkuyh9@gmail.com](mailto:pkuyh9@gmail.com). (B.-P.L.) Telephone: 86 25 52090619. Fax: 86 25 52090616. E-mail: [lbp@seu.edu.cn](mailto:lbp@seu.edu.cn). (P.K.) Telephone: 33 1 56246762. Fax: 33 1 40510636. E-mail: [patrick.keller@curie.fr](mailto:patrick.keller@curie.fr).

### Notes

The authors declare no competing financial interest.

## ACKNOWLEDGMENTS

This research was supported in part by National Natural Science Foundation of China (Grant No. 21002012), Jiangsu Provincial Natural Science Foundation of China (Grant No. BK2011588, BY2011153), and the Fundamental Research Funds for the Central Universities. The authors would like to gratefully thank Prof. Dong-Zhong Chen (Nanjing University) for his help with SAXS experiment measurements.

## REFERENCES

- (1) Dubois, J. C.; LeBarny, P.; Mauzac, M.; Noel, C.; Demus, D.; Goodby, J. W.; Gray, G. W.; Spiess, H. W.; Vill, V., Eds. *Handbook of Liquid Crystals*; VCH: Weinheim, Germany, 1998.
- (2) Hsu, C. S. *Prog. Polym. Sci.* **1997**, *22*, 829–871.
- (3) Chojnowski, J.; Cypryk, M. in *Silicon-Containing Polymers-The Science and Technology of Their Synthesis and Applications*; Jones, R. G.; Ando, W.; Chojnowski, J., Eds.; Springer-Verlag: Dordrecht, The Netherlands, 2000; Chapter 1, 3–35.
- (4) Zheng, P. W.; McCarthy, T. J. *Langmuir* **2011**, *26*, 18585–18590.
- (5) Krumpfer, J. W.; McCarthy, T. J. *Langmuir* **2011**, *27*, 11514–11519.
- (6) Sun, F.; Liao, B.; Zhang, L.; Du, H. G.; Huang, Y. D. *J. Appl. Polym. Sci.* **2011**, *120*, 3604–3612.
- (7) Swinburne, M. L.; Willmot, D.; Patrick, D. *Eur. J. Orthodont.* **2011**, *33*, 407–412.
- (8) Hosseinzadeh, F.; Galehassadi, M.; Mahkam, M. *J. Appl. Polym. Sci.* **2011**, *122*, 2368–2373.
- (9) Mojsiewicz-Pienkowska, K.; Jamrogiewicz, M.; Zebrowska, M.; Sznitowska, M.; Centkowska, K. *J. Pharm. Biomed. Anal.* **2011**, *56*, 131–138.
- (10) Xu, L.; Dai, C. H.; Chen, L.; Xie, H. D. *J. Polym. Eng.* **2011**, *31*, 369–374.
- (11) Finkelmann, H.; Rehage, G. *Makromol. Chem. Rapid Commun.* **1980**, *1*, 31–34.
- (12) Finkelmann, H. *Macromol. Chem.* **1982**, *183*, 1245–1256.
- (13) Kupfer, J.; Finkelmann, H. *Makromol. Chem. Rapid Commun.* **1991**, *12*, 717–726.
- (14) Percec, V.; Rodenhouse, R. *Macromolecules* **1989**, *22*, 4408–4412.
- (15) Percec, V.; Heck, J. *Macromolecules* **1991**, *24*, 4957–4962.
- (16) Percec, V.; Hahn, B. *Macromolecules* **1989**, *22*, 1588–1599.
- (17) Percec, V.; Hahn, B.; Ebert, M.; Wendorff, J. H. *Macromolecules* **1990**, *23*, 2092–2095.
- (18) Percec, V.; Tomazos, D. *Macromolecules* **1989**, *22*, 2062–2069.
- (19) Percec, V.; Tomazos, D. *Macromolecules* **1989**, *22*, 1512–1514.
- (20) Hardouin, F.; Mery, S.; Achard, M. F.; Mauzac, M. *Liq. Cryst.* **1990**, *8*, 565–575.
- (21) Achard, M. F.; Leroux, N.; Hardouin, F. *Liq. Cryst.* **1991**, *10*, 507–517.
- (22) Leroux, N.; Mauzac, M.; Noirez, L.; Hardouin, F. *Liq. Cryst.* **1994**, *16*, 421–428.
- (23) Achard, M. F.; Lecommandoux, S.; Hardouin, F. *Liq. Cryst.* **1995**, *19*, 581–587.

- (24) Lecommandoux, S.; Achard, M. F.; Hardouin, F. *Liq. Cryst.* **1998**, *25*, 85–94.
- (25) Hardouin, F.; Lecommandoux, S.; Achard, M. F. *Kor. Polym. J.* **1998**, *25*, 85–94.
- (26) Lecommandoux, S.; Noirez, L.; Achard, M. F.; Hardouin, F. *Macromolecules* **2000**, *33*, 67–72.
- (27) Frank, B.; Lutz, W.; Michael, H.; Robert, K. *Makromol. Chem.* **1990**, *191*, 1775–1785.
- (28) Guerino, S.; Christopher, K. O.; Terry, B.; Mario, P.; Lupu, A. *J. Polym. Sci., Polym. Chem.* **1995**, *33*, 1913–1916.
- (29) Harshad, P. P.; Jian, L.; Ronald, C. H. *Macromolecules* **2007**, *40*, 6206–6216.
- (30) Zhang, L.-Y.; Chen, S.; Shen, Z.-H.; Chen, X.-F.; Fan, X.-H.; Zhou, Q.-F. *Macromolecules* **2010**, *43*, 6024–6032.
- (31) Zhou, Q. L.; Zhang, J. T.; Ren, Z. J.; Yan, S. K.; Xie, P.; Zhang, R. B. *Macromol. Rapid Commun.* **2008**, *29*, 1259–1263.
- (32) Shenouda, I. G.; Chien, L. C. *Macromolecules* **1993**, *26*, 5020–5023.
- (33) Poths, H.; Andersson, G.; Skarp, K.; Zentel, R. *Adv. Mater.* **1992**, *4*, 792–794.
- (34) Poths, H.; Zentel, R. *Liq. Cryst.* **1994**, *16*, 749–767.
- (35) Kawakami, H.; Mori, Y.; Abe, H.; Nagaoka, S. *J. Membr. Sci.* **1997**, *133*, 245–253.
- (36) Ganicz, T.; Andrzej Stanczyk, W.; Chmielecka, J.; Kowalski, J. *Polym. Int.* **2009**, *58*, 248–254.
- (37) Mukbaniani, O.; Titvinidze, G.; Tatrishvili, T.; Mukbaniani, N.; Brostow, W.; Pietkiewicz, D. *J. Appl. Polym. Sci.* **2007**, *104*, 1176–1183.
- (38) Kade, M. J.; Burke, D. J.; Hawker, C. J. *J. Polym. Sci., Part A: Polym. Chem.* **2010**, *48*, 743–750.
- (39) Franc, G.; Kakkar, A. K. *Chem. Soc. Rev.* **2010**, *39*, 1536–1544.
- (40) Hoyle, C. E.; Bowman, C. N. *Angew. Chem., Int. Ed.* **2010**, *49*, 1540–1573.
- (41) Yang, H.; Buguin, A.; Taulemesse, J. M.; Kaneko, K.; Mery, S.; Bergeret, A.; Keller, P. *J. Am. Chem. Soc.* **2009**, *131*, 15000–15004.
- (42) Campos, L. M.; Killips, K. L.; Sakai, R.; Paulusse, J. M. J.; Damiron, D.; Drockenmuller, E.; Messmore, B. W.; Hawker, C. J. *Macromolecules* **2008**, *41*, 7063–7070.
- (43) Killips, K. L.; Campos, L. M.; Hawker, C. J. *J. Am. Chem. Soc.* **2008**, *130*, 5062–12739.
- (44) Antoni, P.; Robb, M. J.; Campos, L. M.; Montanez, M.; Hult, A.; Malmstrom, E.; Malkoch, M.; Hawker, C. J. *Macromolecules* **2010**, *43*, 6625–6631.
- (45) Cole, M. A.; Bowman, C. A. *J. Polym. Sci., Part A: Polym. Chem.* **2012**, *50*, 4325–4333.
- (46) Campos, L. M.; Meinel, I.; Guino, R. G.; Schierhorn, M.; Gupta, N.; Stucky, G. D.; Hawker, C. J. *Adv. Mater.* **2008**, *20*, 3728–3733.
- (47) Campos, L. M.; Truong, T. T.; Shim, D. E.; Dimitriou, M. D.; Shir, D.; Meinel, I.; Gerbec, J. A.; Hahn, H. T.; Rogers, J. A.; Hawker, C. J. *Chem. Mater.* **2009**, *21*, 5319–5326.
- (48) Yang, H.; Zhang, Q.; Lin, B.-P.; Fu, G.-D.; Zhang, X.-Q.; Guo, L.-X. *J. Polym. Sci., Part A: Polym. Chem.* **2012**, *50*, 4182–4190.
- (49) Kupfer, J.; Finkelmann, H. *Macromol. Chem. Phys.* **1994**, *159*, 1353–1367.
- (50) Buguin, A.; Li, M. H.; Silberzan, P.; Ladoux, B.; Keller, P. *J. Am. Chem. Soc.* **2006**, *128*, 1088–1089.
- (51) Mitsunobu, O. *Synthesis* **1981**, 1–28.
- (52) Neises, B.; Steglich, W. *Angew. Chem.* **1978**, *90*, 556–557.
- (53) Thomsen, D. L., III; Keller, P.; Naciri, J.; Pink, R.; Jeon, H.; Shenoy, D.; Ratna, B. R. *Macromolecules* **2001**, *34*, 5868–5875.
- (54) Fischer, H.; Poser, S.; Arnold, M.; Frank, W. *Macromolecules* **1994**, *27*, 7133–7138.
- (55) Wong, G. C. L.; Commandeur, J.; Fischer, H.; de Jeu, W. H. *Phys. Rev. Lett.* **1996**, *77*, 5221–5224.
- (56) Warner, M.; Terentjev, E. *Liquid Crystal Elastomers*; Oxford University Press: Oxford, U.K., 2003.
- (57) Ikeda, T.; Mamiya, J.; Yu, Y. *Angew. Chem., Int. Ed.* **2007**, *46*, 506–528.
- (58) Ohm, C.; Brehmer, M.; Zentel, R. *Adv. Mater.* **2010**, *22*, 3366–3387.
- (59) de Gennes, P. G. *Phys. Lett. A* **1969**, *28*, 725–726.
- (60) Wu, W.; Yao, L.; Yang, T.; Yin, R.; Li, F.; Yu, Y. *J. Am. Chem. Soc.* **2011**, *133*, 15810–15813.
- (61) Wang, W.; Sun, X.; Wu, W.; Peng, H.; Yu, Y. *Angew. Chem., Int. Ed.* **2012**, *51*, 4644–4647.
- (62) Lehmann, W.; Skupin, H.; Tolksdorf, C.; Gebhard, E.; Zentel, R.; Kruger, P.; Losche, M.; Kremer, F. *Nature* **2001**, *410*, 447–450.
- (63) Kaiser, A.; Winkler, M.; Krause, S.; Finkelmann, H.; Schmidt, A. M. *J. Mater. Chem.* **2009**, *19*, 538–543.
- (64) Yamada, M.; Kondo, M.; Mamiya, J. I.; Yu, Y. L.; Kinoshita, M.; Barrett, C. J.; Ikeda, T. *Angew. Chem., Int. Ed.* **2008**, *47*, 4986–4988.
- (65) Harris, K. D.; Bastiaansen, C. W. M.; Lub, J.; Broer, D. J. *Nano Lett.* **2005**, *5*, 1857–1860.
- (66) van Oosten, C. L.; Bastiaansen, C. W. M.; Broer, D. J. *Nat. Mater.* **2009**, *8*, 677–682.
- (67) Buguin, A.; Li, M.-H.; Silberzan, P.; Ladoux, B.; Keller, P. *J. Am. Chem. Soc.* **2006**, *128*, 1088–1089.
- (68) Wu, Z.; Buguin, A.; Yang, H.; Taulemesse, J. M.; Le Moigne, N.; Bergeret, A.; Wang, X.; Keller, P. *Adv. Funct. Mater.* **2013**, DOI: 10.1002/adfm.201203291.
- (69) Ohm, C.; Serra, C.; Zentel, R. *Adv. Mater.* **2009**, *21*, 4859–4862.
- (70) Yang, H.; Ye, G.; Wang, X.; Keller, P. *Soft Matter* **2011**, *7*, 815–823.
- (71) Ohm, C.; Kapernaum, N.; Nonnenmacher, D.; Giesselmann, F.; Serra, C.; Zentel, R. *J. Am. Chem. Soc.* **2011**, *133*, 5305–5311.
- (72) Fleischmann, E.-K.; Liang, H.-L.; Kapernaum, N.; Giesselmann, F.; Lagerwall, J.; Zentel, R. *Nature Commun.* **2012**, *3*, 1178.
- (73) Ikeda, T.; Nakano, M.; Yu, Y. L.; Tsutsumi, O.; Kanazawa, A. *Adv. Mater.* **2003**, *15*, 201–205.
- (74) Naciri, J.; Srinivasan, A.; Jeon, H.; Nikolov, N.; Keller, P.; Ratna, B. R. *Macromolecules* **2003**, *36*, 8499–8505.
- (75) Yang, H.; Zhang, F.; Lin, B.; Keller, P.; Zhang, X.; Sun, Y.; Guo, L. *J. Mater. Chem. C* **2013**, *1*, 1482–1490.
- (76) Haseloh, S.; Ohm, C.; Smallwood, F.; Zentel, R. *Macromol. Rapid Commun.* **2011**, *32*, 88–93.
- (77) Ohm, C.; Morys, M.; Forst, F. R.; Braun, L.; Eremin, A.; Serra, C.; Stannarius, R.; Zentel, R. *Soft Matter* **2011**, *7*, 3730–3734.
- (78) Rodriguez, I.; Spicar-Mihalic, P.; Kuyper, C. L.; Fiorini, G. S.; Chiu, D. T. *Anal. Chim. Acta* **2003**, *496*, 205–215.